J. Inst. Eng. India Ser. C (February 2017) 98(1):5–15
DOI 10.1007/s40032-016-0271-8

ORIGINAL CONTRIBUTION

Finite Element Simulations of Micro Turning of Ti-6Al-4V using PCD and Coated Carbide tools

Thangavel Jagadesh[1] · **G. L. Samuel**[1]

Received: 25 March 2015 / Accepted: 13 May 2016 / Published online: 8 July 2016

Abstract The demand for manufacturing axi-symmetric Ti-6Al-4V implants is increasing in biomedical applications and it involves micro turning process. To understand the micro turning process, in this work, a 3D finite element model has been developed for predicting the tool chip interface temperature, cutting, thrust and axial forces. Strain gradient effect has been included in the Johnson–Cook material model to represent the flow stress of the work material. To verify the simulation results, experiments have been conducted at four different feed rates and at three different cutting speeds. Since titanium alloy has low Young's modulus, spring back effect is predominant for higher edge radius coated carbide tool which leads to the increase in the forces. Whereas, polycrystalline diamond (PCD) tool has smaller edge radius that leads to lesser forces and decrease in tool chip interface temperature due to high thermal conductivity. Tool chip interface temperature increases by increasing the cutting speed, however the increase is less for PCD tool as compared to the coated carbide tool. When uncut chip thickness decreases, there is an increase in specific cutting energy due to material strengthening effects. Surface roughness is higher for coated carbide tool due to ploughing effect when compared with PCD tool. The average prediction error of finite element model for cutting and thrust forces are 11.45 and 14.87 % respectively.

Keywords Cutting forces · Edge radius · Interface temperature · PCD tool · Coated carbide tool

✉ G. L. Samuel
samuelgl@iitm.ac.in

[1] Department of Mechanical Engineering, Indian Institute of Technology Madras, Chennai 600036, Tamil Nadu, India

Introduction

Titanium alloy has been extensively used in biomedical applications such as, maxillofacial micro-screws, orthopedic, dental, ankle and neuro surgical implants due to its superior properties such as biocompatability, high strength to weight ratio and corrosion resistance [1, 2]. On the other hand, the machining of titanium alloy is a challenging task due to its low elastic modulus, low thermal conductivity and high chemical reactivity with the cutting tool material. Several researchers have proposed different coated tools to reduce the tool wear [3–5]. In this work, PCD tool and coated carbide tool (TiN/AlTiN) have been used to machine the titanium alloy by micro turning. The advantage of the PCD tool is its high thermal conductivity and at high temperature, TiC layer formation will avoid the diffusion of constituents from work material [5]. Whereas coated carbide tool has benefits of low coefficient of friction, high oxidation and wear resistance due to the formation of Al_2O_3 film.

The mechanics of machining at micro scale is different from macro scale due to the size effect. The size effect during micromachining is due to negligible crystal density defect (i.e. vacancy, stacking fault), material separation, strain gradient effect, high strain rate and ploughing mechanism [6–8]. The researchers have reported that material strengthening mechanisms are due to decrease in secondary deformation zone temperature and strain gradient effect [9]. Some of the investigators have developed a model for predicting shear strength and specific shear energy by considering size effect using strain gradient plasticity theory [10]. Earlier, the researchers have reviewed challenges in macro and micro cutting operations and suggested that edge radius, minimum chip thickness, material strengthening due to the size effect are important

considerations in modeling of micro machining process [11].

Experimental investigation of titanium alloy is expensive due to extensive tool wear. So the prediction of forces, tool chip interface temperature, strain, strain rate and in addition to this, understanding the mechanism of material removal and process physics are important. There are different modeling techniques like soft computing, empirical model for predicting the machining process variables. But FEM model is more accurate and commonly used technique to predict the above mentioned parameters that leads to reduced experimental cost [12]. Several researchers have developed finite element models to predict the effect of tool edge radius on tool chip contact length, contact force and chip formation behavior [13, 14]. The researchers have developed finite element model for various edge geometry like chamfer, uniform hone, waterfall hone and variable hone inserts. The results suggested that variable edge geometry has reduced stress concentration, tool wear, heat generation and plastic strain [15].

Several researchers developed finite element models for macro machining of titanium alloy. Some of the researchers have compared the different material models and suggested that flow softening at high strain values in modified Johnson–Cook material model is predicted accurately and matches with experimental values [16]. The investigators have reviewed the importance of material behavior during modeling of metal forming and machining processes [17]. The research group from Rutgers University has developed 2D and 3D finite element model for prediction of tool wear and chip flow during micro milling of titanium alloy. The results suggested that CBN coated tools have reduced the tool wear rate and interface temperature over the carbide tool [18, 19]. Some investigators have developed the coupled thermo mechanical numerical analysis during micro milling of bio-medical implant. Results reveal that preheating of workpiece material ahead of cutting tool has a better finish with less burr formation [20].

In prior literature, the finite element simulation has been developed for macro machining process. There is no attempt has made so far on the effect of edge radius on the forces and tool chip temperature during micro turning of titanium alloy. In this work, to get the actual cutting process, 3D finite element model has been developed by incorporating edge radius and strain gradient effects. The main focus of this work is to understand, the mechanism of material removal at the micro scale and the influence of edge radius on forces, tool chip temperature. Finally, the model is validated with different experimental cutting conditions. Besides this, the surface roughness and chip morphology has been analyzed with different feed rates.

Methodology

Finite Element Model

Finite element simulation is carried out by using commercially available software DEFORM 3D. Lagrangian formulation with implicit integration method is used for the simulation in which chip formation is achieved by adaptive re-meshing technique. In the case of the finite element simulation of machining process, the prediction of process variables mainly depends on the friction and material model.

Workpiece Material Model

In the present investigation, Johnson and Cook material model is used for the prediction of the flow stress, which is the function of strain, strain rate and temperature as shown in Eq. 1a [21],

$$\sigma = [A + B \in^{n}]\left[1 + C \ln \frac{\dot{\epsilon}}{\dot{\epsilon}_0}\right]\left[1 - \left(\frac{T - T_o}{T_m - T_o}\right)^{m}\right] \qquad (1a)$$

where A = yield strength of the material; B = strain hardening modulus; C = strain rate sensitivity coefficient; ε = plastic strain; $\dot{\varepsilon}$ = strain rate; $\dot{\varepsilon}_0$ reference plastic strain rate; T = work piece temperature; T_m = melting temperature; T_o = room temperature; m = thermal softening coefficient; n = Hardening coefficient. There are different Johnson and Cook material parametric values for Ti-6Al-4V proposed by several researchers. Some researchers have suggested that Lee and Lin parametric values are in good agreement with the experimental values during macro machining of titanium alloy [22]. So in this work, Lee and Lin [23] constants are included in Johnson and Cook material model during micro machining of titanium alloy which are given in Table 1 [23, 24]. The models which are used for macro machining process cannot be used for micro machining due to the size effect. The researchers have modified the Johnson–Cook material model with strain gradient plasticity to represent the flow stress of the work material as shown in Eq. 1b [25],

Table 1 Johnson–Cook parameters of Ti-6Al-4V [20, 23, 24]

Parameters	A, MPa	B, MPa	C	n	m	T_{melt}, °C	b, nm	a	χ	G, GPa
Values	782.7	498.4	0.028	0.28	1	1660	0.295	0.5	0.38	44

$$\sigma_{micro} = \sigma\sqrt{1 + \left(\frac{18ab^2G^2}{\sigma^2}\right)^{\chi}} \quad (1b)$$

where σ_{micro} = flow stress of work material; G = shear modulus; b = magnitude of burger vector; a = empirical constant; χ = geometric dislocation density and σ = effective strain gradient. The effective strain gradient is calculated using Eq. 1c [26],

$$\sigma = \frac{2\cos_n}{\sqrt{3}s_0\cos(\varphi_n - {}_n)\sin\varphi_n} \quad (1c)$$

where σ = effective strain gradient; n = normal rake angle; φ_n = normal shear angle and s_0 is the thickness of primary shear zone which is taken as 0.5 times of uncut chip thickness [27].

Workpiece is assumed as viscoplastic material and 100,659 tetrahedron elements are used to model the workpiece material. The shape of the element is four node tetrahedron element. The numbers of nodes per element are 6 and each node has three degrees of freedom. The minimum element size of the workpiece is considered as 2 μm in all simulation conditions. Figure 1(a) shows the variation of flow stress with strain for different constitutive models. Model 3 shown in Fig. 1a starts at high flow stress value when compared with other two models. This is due to strain gradient effect which is predominant for low value of strain, depth of cut and uncut chip thickness. Figure 1b shows the variation of flow stress with strain at various temperatures obtained using Johnson–Cook material model with strain gradient plasticity.

Cutting Tool Model

Cutting insert is modelled using solid works software and imported in DEFORM 3D software. To get the influence of edge radius a fine mesh density is given at the tip of the tool and coarse mesh at the remaining place, as shown in Fig. 2a. The number of elements used to model the tool are 68,963. Figure 2b shows coating of AlTiN and TiN over carbide tool. The thickness of the coating is 10 μm.

Table 2 shows the thermo mechanical properties of tool and workpiece material [3, 4, 28, 29]. Table 3 shows the variation of flow stress with strain at various temperature. Workpiece is fixed at the bottom portion in x, y and z directions and the tool is considered as rigid as shown in Fig. 2c.

Friction Modeling

Shear friction law ($\tau = mk$) and coulomb friction law ($\tau = \mu p$) are used to represent the friction between tool and chip interface in the finite element modeling. If $\mu p \leq mk$, then it is considered as sliding friction, otherwise it is considered as sticking friction. Deform 3D automatically detect the contact conditions for an element.

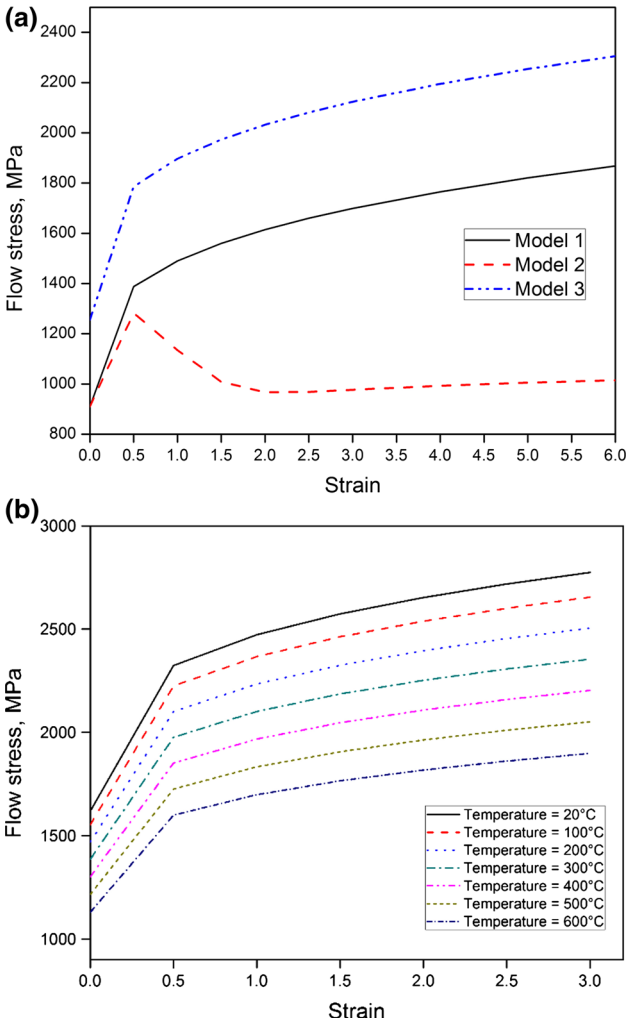

Fig. 1 Variation of flow stress with strain. **a** Variation of flow stress with strain with different models. *Model 1* Johnson–Cook material model [21]. *Model 2* Modified Johnson–Cook material model with strain softening at high strain values [16]. *Model 3* Modified Johnson–Cook material model with strain gradient plasticity. **b** Variation of flow stress with strain at various temperatures with 10^4/s strain rate *Model 3*

$$m = \frac{\tau}{k} \quad (2)$$

where m = shear friction factor; τ = frictional shear stress; k = work material flow stress.

A sensitive analysis has been done and finally constant shear friction factor $m = 0.95$ is used in all simulation conditions as suggested by earlier researchers [3]. The formula for calculating shear friction factor is shown in Eq. 2, and specific cutting energy is shown in Eq. 3.

$$\text{Specific cutting energy} = \frac{Fc \times Vc}{DOC \times Vc \times f} \quad (3)$$

where Fc = Cutting force; Vc = Cutting speed; DOC = Depth of cut; f = feed rate.

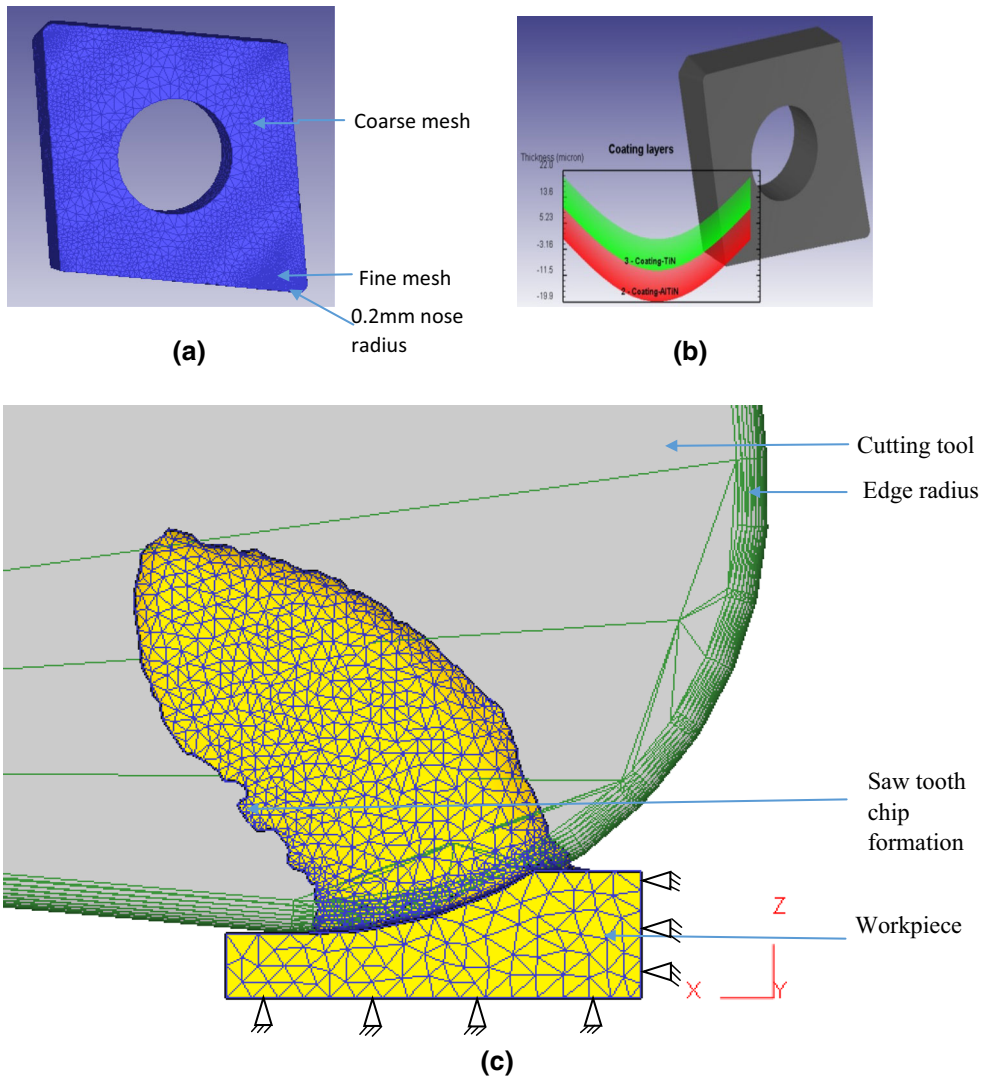

Fig. 2 Finite element simulation during micro turning of titanium alloy. **a** Cutting insert. **b** Coated carbide tool. **c** Finite element model along with chip formation

Table 2 Mechanical and thermal properties of tool and work material [Temperature (T), °C]

Property	Ti-6Al-4V [3]	WC–Co [3]	AlTiN [3, 4]	TiN [3, 29]	PCDtool [28]
Youngs modulus, MPa	$(0.7412 \times T) + 113{,}375$	5.0×10^5	560×10^3	251×10^3	1,050,000
Thermal conductivity, W/m °C	$7.039 \times 10^{(0.0011 \times T)}$	$(0.042 \times T) + 36$	$(0.0081 \times T) + 11.95$	$(0.008 \times T) + 19.8$	1000
Thermal expansion, mm/mm °C	$(3.1 \times 10^{-9} \times T) + (7.1 \times 10^{-6})$	4.7×10^{-6}	9.4×10^{-6}	9.4×10^{-6}	2.5×10^{-6}
Heat capacity, N/mm^2 °C	$2.24 \times 10^{(0.0007 \times T)}$	$(0.0005 \times T) + 2.07$	$(0.0003 \times T) + 0.57$	3.00	1.26
Poisson's ratio	0.34	0.25	0.25	0.25	0.1

Thermal Boundary Conditions

Ambient temperature is taken as 20 °C. The convective heat transfer coefficient during the process is taken as 0.02 N/Sec/mm/ °C and the heat transfer coefficient between tool and work piece interface is taken as 10^7 N/Sec/mm/ °C [30].

Experimental Setup

Micro turning experiments have been carried out with varying cutting conditions and the closer view of the experimental setup is shown in Fig. 3. The workpiece material is Titanium alloy (Ti-6Al-4V) of grade 5. The coated carbide tool (060202 TT5080) and the PCD (060202

Table 3 Variation of flow stress with strain at various temperatures at strain rate of 10^4/s

Sl. no	Flow stress, MPa							
	Strain	T °C						
		20	100	200	300	400	500	600
1	0	1619.94	1553.31	1469.66	1385.53	1300.87	1215.61	1129.64
2	0.5	2324.04	2225.25	2101.36	1976.96	1851.98	1726.33	1599.90
3	1	2472.76	2367.113	2234.63	2101.63	1968.04	1833.77	1698.72
4	1.5	2573.80	2463.48	2325.15	2186.30	2046.85	1906.71	1765.78
5	2	2652.62	2538.64	2395.74	2252.32	2108.29	1963.57	1818.06
6	2.5	2718.18	2601.16	2454.46	2307.22	2159.38	2010.85	1861.51
7	3	2774.81	2655.15	2505.16	2354.63	2203.50	2051.66	1899.02

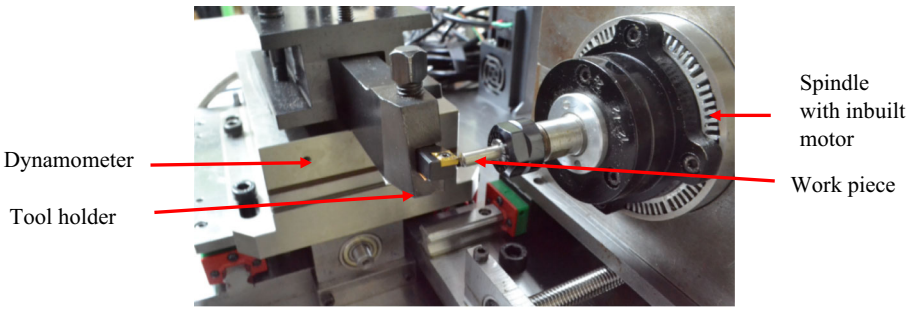

Fig. 3 Closer view of micro turning setup

Table 4 Comparison of experimental and simulated cutting force for PCD and coated carbide tool

Sl. no.	Parameters			Cutting tool	Cutting force, N		Prediction error, %
	Cutting speed, m/min	Feed, µm/rev	Depth of cut, µm		Experimental results	Finite element model	
1	19	20	30	PCD	9.14	11.35	−24.18
2	38	20	30	PCD	8.29	8.53	−2.90
3	57	20	30	PCD	7.23	8.50	−17.57
4	75	20	30	PCD	6.70	7.60	−13.43
5	19	20	30	Coated	11.41	11.62	−1.84
6	38	20	30	Coated	9.69	8.76	9.60
7	57	20	30	Coated	7.99	7.75	3.00
8	75	20	30	Coated	8.55	7.18	16.02
9	19	5	30	PCD	3.23	2.34	27.55
10	19	10	30	PCD	5.87	5.93	−1.02
11	19	15	30	PCD	6.57	7.22	−9.89
12	19	5	30	Coated	5.16	5.07	1.74
13	19	10	30	Coated	8.98	6.96	22.49
14	19	15	30	Coated	9.65	8.77	9.12

KP300) tool of Tague tech make has been selected as a tool material. The insert tool holder [SCLCR 0808 K06 – Taegu Tech) has approach and clearance angles of 95° and 6° respectively. The forces were measured by using a kistler piezo electric dynamometer (9257 b). It has a sensitivity of 7.5, 3.5 and 3.5 pCN in the cutting (F_z), thrust (F_y) and axial (F_x) directions respectively.

To validate the FEM results, experiments have been carried out by varying feed rates and cutting speeds at fixed depth of cut. The comparisons of cutting, thrust, and axial

Table 5 Comparison of experimental and simulated thrust force for PCD and coated carbide tool

Sl. no.	Parameters			Cutting tool	Thrust force, N		Prediction error, %
	Cutting speed, m/min	Feed, μm/rev	Depth of cut, μm		Experimental results	Finite element model	
1	19	20	30	PCD	6.36	6.29	1.10
2	38	20	30	PCD	4.72	4.48	5.08
3	57	20	30	PCD	6.24	4.82	22.76
4	75	20	30	PCD	3.32	3.70	−11.45
5	19	20	30	Coated	11.23	9.47	15.67
6	38	20	30	Coated	9.35	7.56	19.14
7	57	20	30	Coated	7.34	6.85	6.68
8	75	20	30	Coated	7.02	6.96	0.85
9	19	5	30	PCD	2.75	1.57	42.91
10	19	10	30	PCD	3.08	4.77	−54.87
11	19	15	30	PCD	4.15	3.74	9.88
12	19	5	30	Coated	5.57	5.56	0.18
13	19	10	30	Coated	5.83	6.54	−12.18
14	19	15	30	Coated	6.96	7.34	−5.46

Table 6 Comparison of experimental and simulated feed force for PCD and coated carbide tool

Sl. no.	Parameters			Cutting tool	Feed force, N		Prediction error, %
	Cutting speed, m/min	Feed, μm/rev	Depth of cut, μm		Experimental results	Finite element model	
1	19	20	30	PCD	1.76	1.71	2.84
2	38	20	30	PCD	1.40	1.25	10.71
3	57	20	30	PCD	1.21	1.36	−12.40
4	75	20	30	PCD	1.26	1.09	13.49
5	19	20	30	Coated	3.60	2.70	25.00
6	38	20	30	Coated	3.34	2.66	20.36
7	57	20	30	Coated	2.90	2.47	14.83
8	75	20	30	Coated	2.40	1.96	18.33
9	19	5	30	PCD	2.39	0.51	78.66
10	19	10	30	PCD	2.76	1.49	46.01
11	19	15	30	PCD	2.06	1.12	45.63
12	19	5	30	Coated	2.39	1.64	31.38
13	19	10	30	Coated	2.41	1.88	21.99
14	19	15	30	Coated	3.12	2.09	33.01

forces during experimental and FEM simulations are shown in Table 4, 5 and 6.

Results and Discussion

Finite Element Model Validation

Finite element simulation results are validated with experimental cutting, thrust and axial forces. Figure 4a, b show the typical comparison of experimental and simulated cutting and thrust forces when machined using PCD tool.

Fig. 4 Comparison of experimental results with finite element model. ▶ **a** Comparison of simulated and experimental cutting force at 38 m/min cutting speed, 20 μm/rev feed and 30 μm depth of cut. **b** Comparison of simulated and experimental thrust force at 38 m/min cutting speed, 20 μm/rev feed and 30 μm depth of cut. **c** Variation of forces with cutting speed during micro turning using PCD tool. **d** Variation of forces with cutting speed during micro turning using coated carbide tool. **e** Effective stress distribution during micro turning simulation using PCD tool at 38 m/min cutting speed, 30 μm depth of cut and 20 μm/rev feed. **f** Effective stress distribution during micro turning simulation using coated carbide tool at 38 m/min cutting speed, 30 μm depth of cut and 20 μm/rev feed. **g** Variation of forces with feed rates during micro turning using diamond tool. **h** Variation of forces with feed rates during micro turning using coated carbide tool

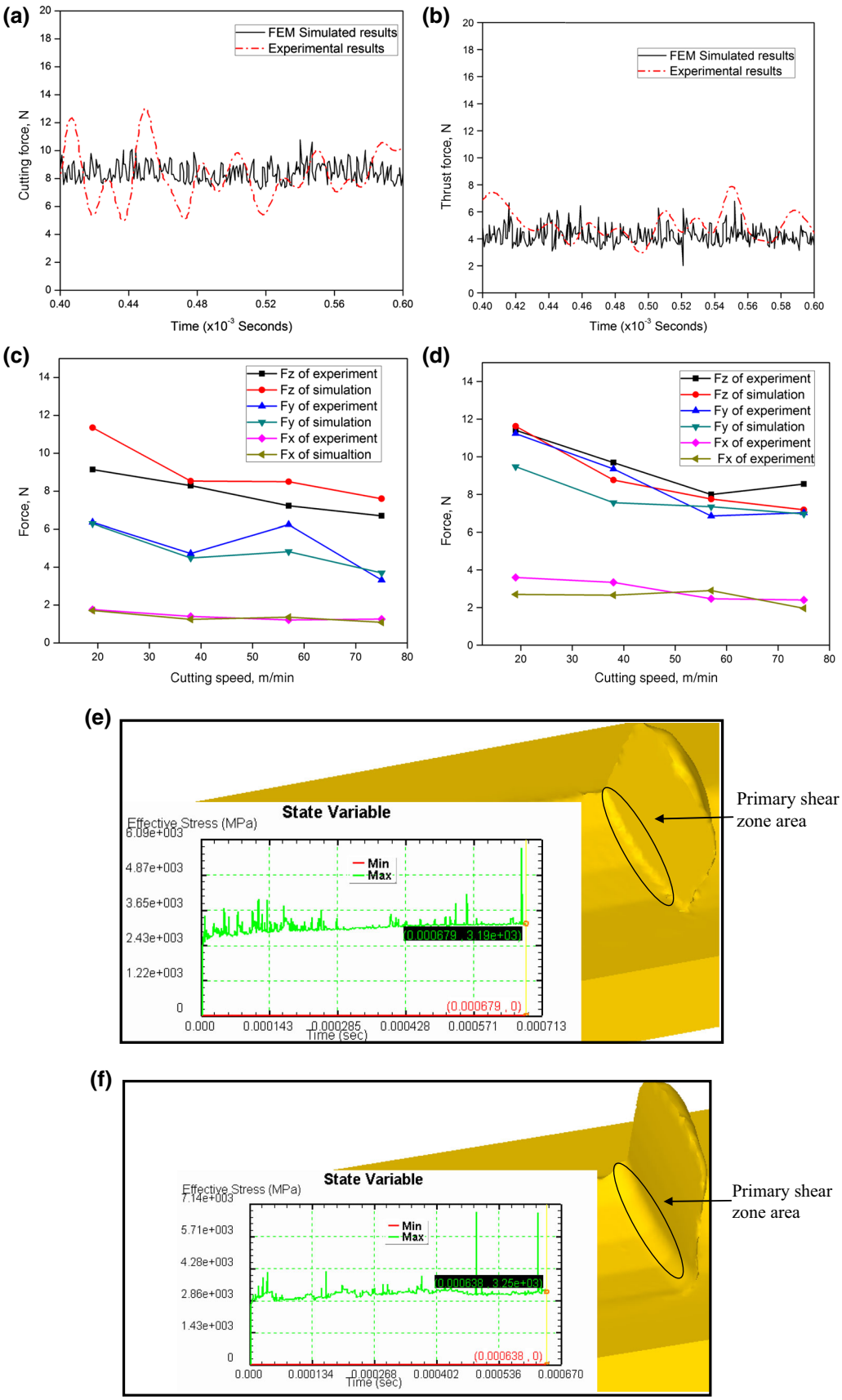
(a)
FEM Simulated results
Experimental results
Cutting force, N
Time (x10-3 Seconds)
(b)
FEM Simulated results
Experimental results
Thrust force, N
Time (x10-3 Seconds)
(c)
Fz of experiment
Fz of simulation
Fy of experiment
Fy of simulation
Fx of experiment
Fx of simualtion
Force, N
Cutting speed, m/min
(d)
Fz of experiment
Fz of simulation
Fy of experiment
Fy of simulation
Fx of experiment
Fx of experiment
Force, N
Cutting speed, m/min
(e)
State Variable
Effective Stress (MPa)
Min
Max
Time (sec)
Primary shear zone area
(f)
State Variable
Effective Stress (MPa)
Min
Max
Time (sec)
Primary shear zone area

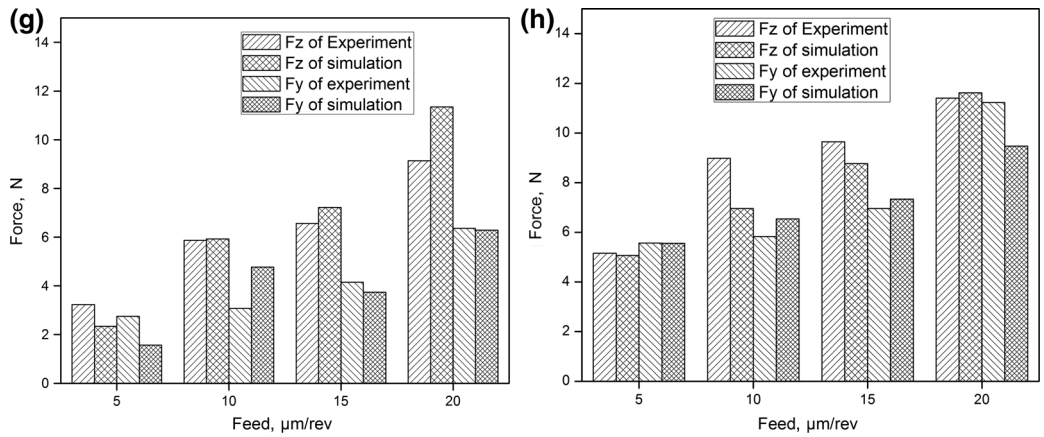

Fig. 4 continued

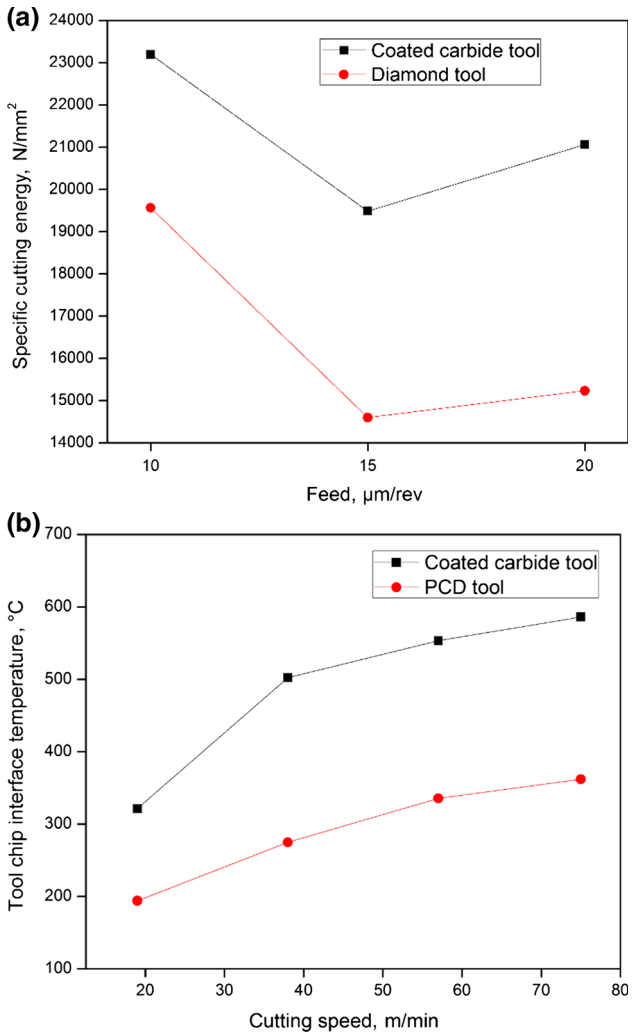

Fig. 5 Variation of tool chip interface temperature and specific cutting energy with cutting speed and feed rate. **a** Variation of specific cutting energy with feed rate. **b** Variation of tool chip interface temperature with cutting speed

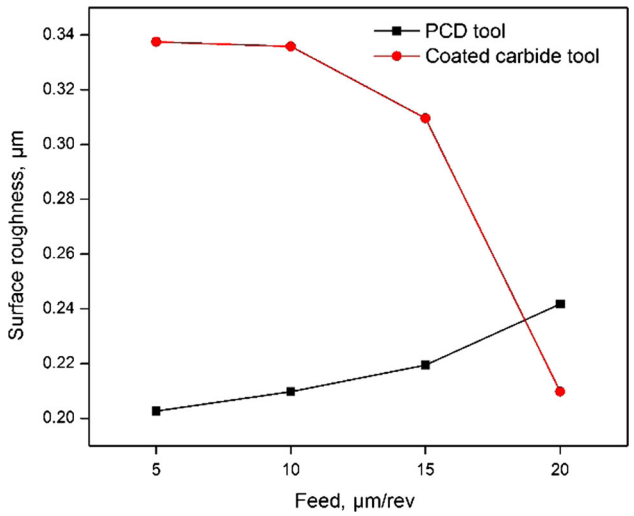

Fig. 6 Variation of surface roughness with feed rate at 19 m/min cutting speed, 20 μm/rev feed and 30 μm depth of cut

The average experimental cutting and thrust forces are 8.29 and 4.72 N respectively at 38 m/min cutting speed and 30 μm depth of cut with prediction error of 2.90 and 5.80 % respectively.

From the experimental investigation it is observed that, when cutting speed increases from 19 to 75 m/min there is a decrease in the cutting force from 11.41 to 8.55 N and from 9.14 to 6.7 N by using coated carbide and diamond tool respectively as shown in Fig. 4c, d. The reason for decrease in the cutting force is due to an increase of interface temperature in the cutting zone. As cutting speed increases, magnitude of cutting and thrust force almost equal during micro turning of titanium alloy by coated carbide tool due to spring back effect which is predominant for higher edge radius. Similar trend is observed in both experiment and finite element simulation results. The

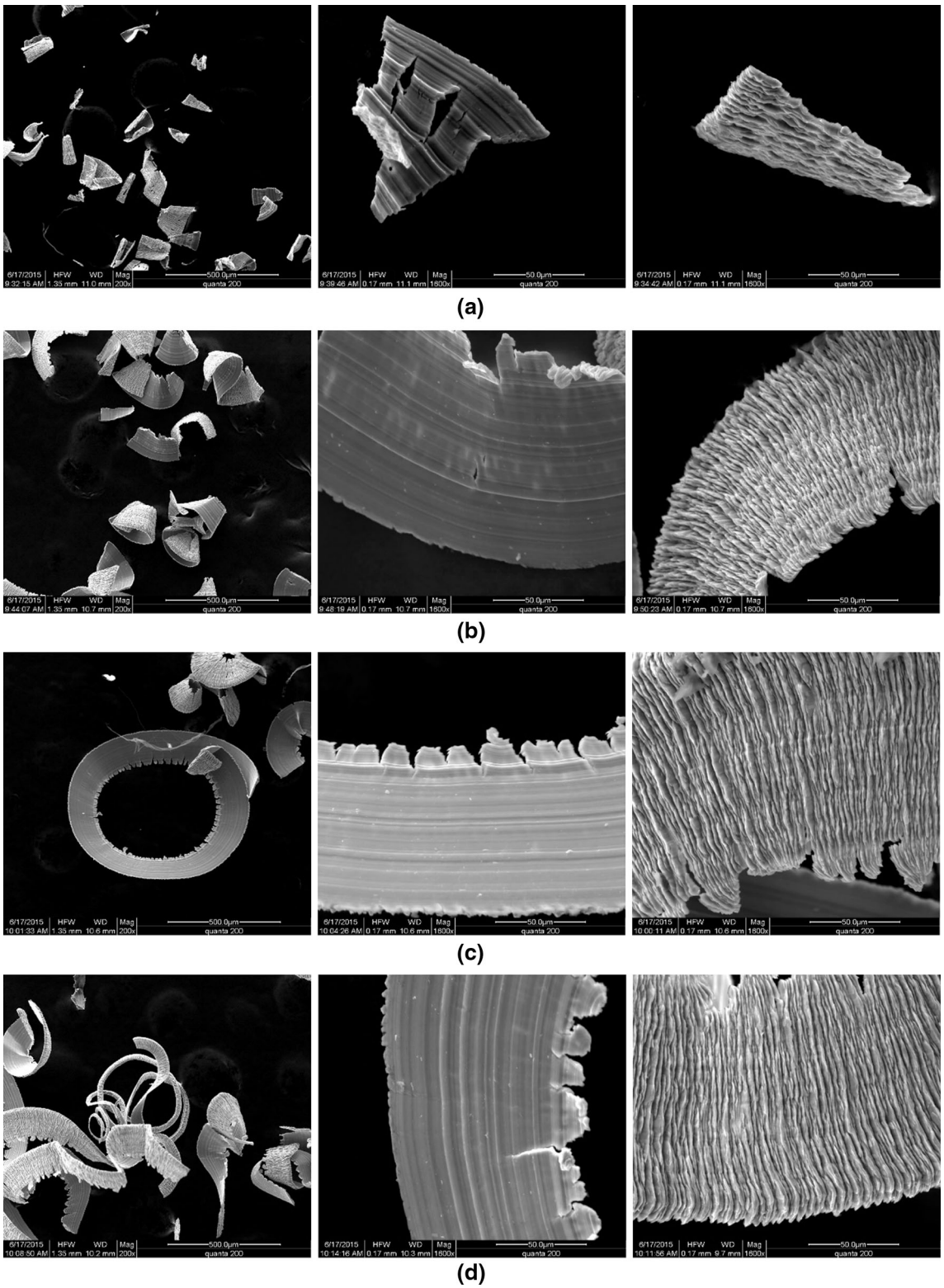

Fig. 7 Chip morphology at different feed rates. **a** Chip morphology machined at 19 m/min cutting speed, 30 μm depth of cut and 5 μm/rev feed. **b** Chip morphology machined at 19 m/min cutting speed, 30 μm depth of cut and 10 μm/rev feed. **c** Chip morphology machined at 19 m/min cutting speed, 30 μm depth of cut and 15 μm/rev feed. **d** Chip morphology machined at 19 m/min cutting speed, 30 μm depth of cut and 20 μm/rev feed

coated carbide tool has higher edge radius of 15 μm as compared to diamond tool 2 μm which results in higher cutting forces due to increase of contact area and high effective stress distribution as shown in Fig. 4e, f.

Cutting force increases with the increase of feed rate due to increased volume of material removal in both experiments and finite element simulations as shown in Fig. 4g, h. High discrepancy between experiment and finite element analysis (FEA) feed forces are due to edge radius of the tool and the influence of the spindle run out at low feed rates. Figure 5a shows the variation of specific cutting energy at various feed rates. When uncut chip thickness decreases, there is an increase in specific cutting energy due to material strengthening effects.

Effect of Interface Temperature on Cutting Speed

Figure 5b shows the variation of tool chip interface temperature with cutting speed. Since titanium alloy has low thermal conductivity, heat generated during machining is not dissipated, and hence there is an increase of tool chip temperature with cutting speed. PCD tool dissipates quickly of heat when compared to coated carbide tool. Hence the tool chip interface temperature is less in PCD tool.

Surface Roughness

Figure 6 shows the variation of surface roughness with feed rates during micro turning of titanium alloy by using PCD and coated carbide tools. Surface roughness mainly depends on the edge radius of the tool during micro turning process. It has been clearly observed that coated carbide tool shows poor surface finish when uncut chip thickness is less than the edge radius whereas PCD tool has sharp cutting edge which leads to good surface finish at lower feed rates.

Chip Morphology

Chip morphology has been analysed at different feed rates from 5 to 20 μm/rev, 19 m/min cutting speed, 30 μm depth of cut and is shown in Fig. 7. Discontinuous chips are observed at lower feed rates and at higher magnification it shows the evidence of fracture of chips as shown in Fig. 7a, b. When the feed rate increases from 5 to 20 μm/rev, there is a change in chip formation mode from discontinuous to continuous curled chips. During machining of titanium alloy, strain gets localized in the shear zone and instability exists in the plastic flow of work piece material which leads to saw tooth formation. The saw tooth formation is predominant at higher feed rate due to increased temperature in cutting zone and can be clearly seen in Fig. 7c, d. The reason for the saw tooth chip formation in machining of titanium alloy is due to adiabatic shear sensitivity or cyclic crack initiation and propagation [31].

Conclusion

In this study, 3D oblique FEM has been developed by considering the edge radius and material strengthening effects to get the accurate prediction of the cutting forces during micro turning of titanium alloy. Cutting edge radius plays a critical role in the magnitude of forces and surface roughness. When uncut chip thickness is less than the edge radius, material is removed by rubbing or ploughing action which leads to an increase in the specific cutting energy and surface roughness. The energy consumed to remove the material by PCD tool is lower as compared to coated carbide tool due to smaller edge radius. Interface heat generation is predominant at high speed, which leads to decrease in forces. PCD tool shows lower interface temperature at higher speed as compared to coated carbide tool due to high thermal conductivity.

The future scope of this work is to compare the chip morphology and tool wear of PCD and coated carbide tool, and to do an optimization study of the machining parameters to get better surface finish and less energy consumption.

References

1. H.J. Rack, J.I. Qazi, Titanium alloys for biomedical applications. Mater. Sci. Eng. C **26**(8), 1269–1277 (2006)
2. V.K. Jain, *Micromanufacturing Processes* (Taylor & Francis, Boca Raton, London, New York, 2012)
3. T. Özel, M. Sima, A.K. Srivastava, B. Kaftanoglu, Investigations on the effects of multi-layered coated inserts in machining Ti-6Al-4V alloy with experiments and finite element simulations. CIRP Ann. Manuf. Technol. **59**(1), 77–82 (2010)
4. S.I. Jaffery, P. Mativenga, Wear mechanisms analysis for turning Ti-6Al-4V—towards the development of suitable tool coatings. Int. J. Adv. Manuf. Technol. **58**(5–8), 479–493 (2012)
5. P.D. Hartung, B.M. Kramer, B.F. von Turkovich, Tool wear in titanium machining. CIRP Ann. Manuf. Technol. **31**(1), 75–80 (1982)
6. M. Shaw, The size effect in metal cutting. Sadhana **28**(5), 875–896 (2003)
7. S. Subbiah, S.N. Melkote, Effect of finite edge radius on ductile fracture ahead of the cutting tool edge in micro-cutting of Al2024-T3. Mater. Sci. Eng. A **474**(1–2), 283–300 (2008)
8. E.J.A. Armarego, R.H. Brown, On the size effect in metal cutting. Int. J. Prod. Res. **1**(3), 75–99 (1961)
9. K. Liu, S.N. Melkote, Material strengthening mechanisms and their contribution to size effect in micro-cutting. J. Manuf. Sci. Eng. **128**(3), 730–738 (2005)
10. S.S. Joshi, S.N. Melkote, An explanation for the size-effect in machining using strain gradient plasticity. J. Manuf. Sci. Eng. **126**(4), 679–684 (2005)

11. M.S. Shunmugam, Machining challenges: macro to micro cutting. J. Inst. Eng. Ser. C **97**(2), 223–241 (2015)
12. P.M. Dixit, U.S. Dixit, *Modeling of metal forming and machining processes: by finite element and soft computing methods* (Springer, London, 2008)
13. K.S. Woon, M. Rahman, K.S. Neo, K. Liu, The effect of tool edge radius on the contact phenomenon of tool-based micromachining. Int. J. Mach. Tools Manuf. **48**(12–13), 1395–1407 (2008)
14. K. Woon, M. Rahman, The effect of tool edge radius on the chip formation behavior of tool-based micromachining. Int. J. Adv. Manuf. Technol. **50**(9–12), 961–977 (2010)
15. T. Özel, Computational modelling of 3D turning: influence of edge micro-geometry on forces, stresses, friction and tool wear in PcBN tooling. J. Mater. Process. Technol. **209**(11), 5167–5177 (2009)
16. M. Sima, T. Özel, Modified material constitutive models for serrated chip formation simulations and experimental validation in machining of titanium alloy Ti-6Al-4V. Int. J. Mach. Tools Manuf. **50**(11), 943–960 (2010)
17. U.S. Dixit, S.N. Joshi, J.P. Davim, Incorporation of material behavior in modeling of metal forming and machining processes: a review. Mater. Des. **32**(7), 3655–3670 (2011)
18. T. Özel, T. Thepsonthi, D. Ulutan, B. Kaftanoğlu, Experiments and finite element simulations on micro-milling of Ti-6Al-4V alloy with uncoated and cBN coated micro-tools. CIRP Ann. Manuf. Technol. **60**(1), 85–88 (2011)
19. T. Thepsonthi, T. Özel, 3-D finite element process simulation of micro-end milling Ti-6Al-4V titanium alloy: experimental validations on chip flow and tool wear. J. Mater. Process. Technol. **221**, 128–145 (2015)
20. N. Shen, H. Ding, Thermo-mechanical coupled analysis of laser-assisted mechanical micromilling of difficult-to-machine metal alloys used for bio-implant. Int. J. Precis. Eng. Manuf. **14**(10), 1677–1685 (2013)
21. G.R. Johnson, W.H. Cook, Fracture characteristics of three metals subjected to various strains, strain rates, temperatures and pressures. Eng. Fract. Mech. **21**(1), 31–48 (1985)
22. D. Umbrello, Finite element simulation of conventional and high speed machining of Ti6Al4V alloy. J. Mater. Process. Technol. **196**(1–3), 79–87 (2008)
23. W.-S. Lee, C.-F. Lin, High-temperature deformation behaviour of Ti6Al4V alloy evaluated by high strain-rate compression tests. J. Mater. Process. Technol. **75**(1–3), 127–136 (1998)
24. I. Asm, *Materials and coatings for medical devices: cardiovascular* (ASM International, Materials Park, Ohio, USA, 2009)
25. X. Lai, H. Li, C. Li, Z. Lin, J. Ni, Modelling and analysis of micro scale milling considering size effect, micro cutter edge radius and minimum chip thickness. Int. J. Mach. Tools Manuf. **48**(1), 1–14 (2008)
26. N. Tounsi, J. Vincenti, A. Otho, M.A. Elbestawi, From the basic mechanics of orthogonal metal cutting toward the identification of the constitutive equation. Int. J. Mach. Tools Manuf. **42**(12), 1373–1383 (2002)
27. S. Rao, M.S. Shunmugam, Analytical modeling of micro end-milling forces with edge radius and material strengthening effects. Mach. Sci. Technol. **16**(2), 205–227 (2012)
28. T. Moriwaki, A. Horiuchi, K. Okuda, Effect of cutting heat on machining accuracy in ultra-precision diamond turning. CIRP Ann. Manuf. Technol. **39**(1), 81–84 (1990)
29. Y.C. Yen, A. Jain, P. Chigurupati, W.T. Wu, T. Altan, Computer simulation of orthogonal cutting using a tool with multiple coatings. Mach. Sci. Technol. **8**(2), 305–326 (2004)
30. T. Thepsonthi, T. Özel, Finite element simulation of micro-end milling titanium alloy: comparison of viscoplastic and elasto-viscoplastic models. Proc. NAMRI/SME **41**, 350–357 (2013)
31. Z.P. Wan, Y.E. Zhu, H.W. Liu, Y. Tang, Microstructure evolution of adiabatic shear bands and mechanisms of saw-tooth chip formation in machining Ti6Al4V. Mater. Sci. Eng. A **531**, 155–163 (2012)